19e Journées de l'Hydrodynamique
26 – 28 novembre 2024, Nantes

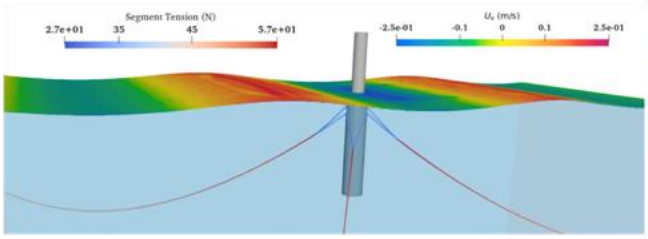

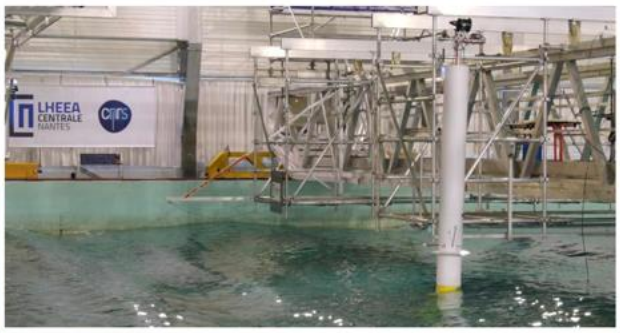

VALIDATION OF A NEW SEAKEEPING SOLUTION FOR THE FORWARD SPEED PROBLEM USING FULL SCALE MEASUREMENT ABOARD A CONTAINER SHIP

Jérôme de LAUZON[(1)], Minh Quan NGUYEN[(1)], Alexandru ANDONIU[(1)]
jerome.de-lauzon@bureauveritas.com ; minh-quan.nguyen@bureauveritas.com ; alexandru.andoniu@bureauveritas.com

[(1)] Bureau Veritas Marine & Offshore, Research Department

Summary

The consistent solution of the seakeeping problem for a ship with constant forward speed in waves is much more complicated than the solution for a stationary floating unit. A new solution has recently been proposed by Chen et al. [1], and the corresponding quasi-static hydro-structure interface introduced in Nguyen et al. [2] makes it possible to consistently compute stresses on ships advancing with constant forward speed in waves.

In this article, the stresses measured aboard a 9400 TEUs container ship are used to validate the new forward speed solution: after retrieving the wave data from the ERA 5 hindcast database along the ship routes, the short-term stresses are computed from the stress transfer functions using spectral analysis, and the results are compared with the measured stresses in terms of standard deviations and accumulated fatigue damage.

The results obtained with the new solution are also compared with the former solution using the so-called encounter frequency approximation, and an in-depth analysis is performed to understand the reasons of the differences observed.

I – Introduction

Between 2006 and 2009, the CMA CGM Rigoletto, a 9400 TEU container ship, was equipped with a monitoring system measuring the structural response. The data was collected during the Lashing@Sea joint industry project and then the TULCS (Tools for Ultra Large Container Ships) European project [3]. In 2012, within the CRS (Cooperative Research Ships) framework, the data was then collected and synchronized to make it easily accessible by the members of CRS.

Over the past four years, the data has been used within CRS to validate the concept of "virtual hull structure monitoring", which aims at monitoring the stresses in the structure using pre-computed stress transfer functions and hindcast metocean data. Until recently, the stress transfer functions were always obtained using a classic hydro-structure interface between a finite element solver and a potential flow solver based on the encounter frequency approach [4].

In parallel, new methods to consistently solve the seakeeping problem have been investigated and resulted in a new solution, using boundary integration equation method based on the Kelvin type of Green's function. The detail of this solution has already been presented in [1], as well as its interfacing with a finite element solver to be able to compute stress transfer functions ([2]).

In this study, full-scale experimental data is used to validate the hydro-structure computations based on the hydrodynamic pressures computed by this new seakeeping solution. The comparison with the encounter frequency solution is also shown.

II – Instrumentation of CMA-CGM Rigoletto

II – 1 Overview

The instrumentation of the ship is mainly focused on the structural behavior, but it also includes the navigation parameters (position, forward speed, draft, transverse metacentric height), accelerations measured along the ship, as well as global motions of the ship (surge, sway, heave, roll, pitch and yaw). In this study, the focus is set on the structural response, and the description of the strain gauges is detailed in the next two paragraphs.

II – 2 Long base strain gauges

The ship is equipped with 8 long base strain gauges (LBSG), intended to measure global strains. These sensors consist of 2 meters steel rods, clamped at one end; displacement is measured at the other end using an electronic micrometer (see Figure 1).

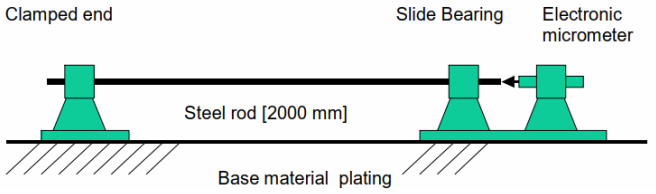

Figure 1. Long base strain gauge

The LBSGs are in frames 75 and 100 and placed in longitudinal direction, as shown in Figure 2. For each frame, two LBSGs are located at deck level, and two at the bottom of the cargo hold.

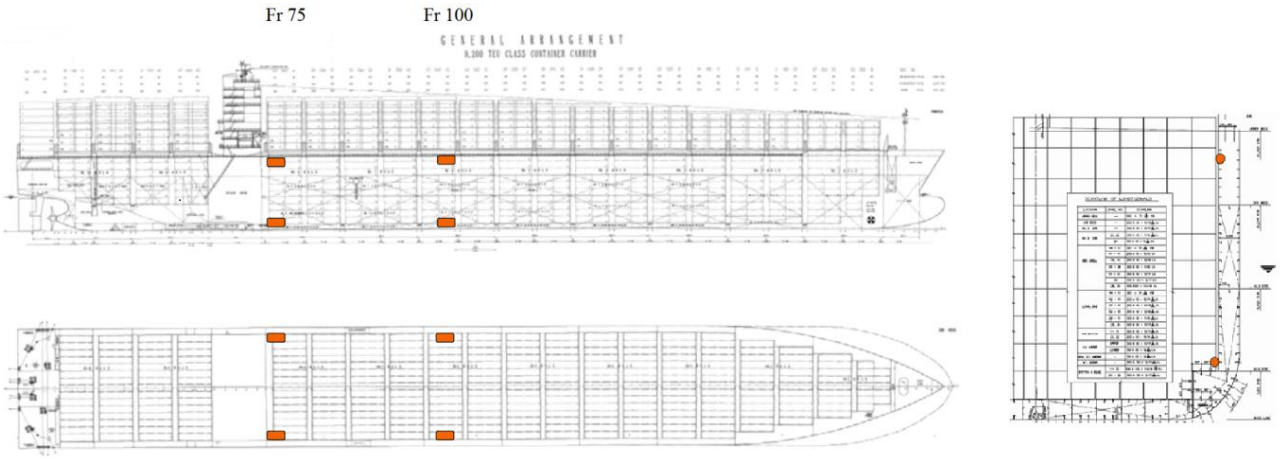

Figure 2. Position of long base strain gauges

II – 3 Local strain gauges

Among all the local strain gauges fitted on the ship, the focus of this study is on the strain gauges installed at the hatch corners, located at the connection between the main deck and the engine room bulkhead. This structural detail is typically subjected to high stress levels, so being able to accurately predict its structural response is of paramount importance. On portside and starboard, three strain gauges are fitted on the edges, as shown in Figure 3:

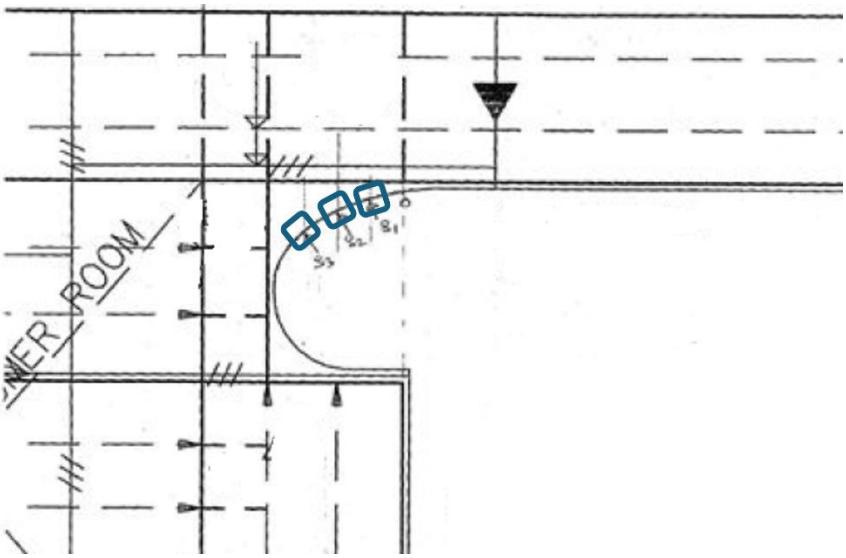

Figure 3. Position of strain gauges on the hatch corners

.

III – Numerical modeling

III – 1 Finite element modeling

The coarse mesh of the ship was provided by HHI. It contains 83 600 elements with typical element size between 2 and 3 meters. Structural elements are represented with plates and bars while containers and ballast loading are represented using mass points and rigid elements. The loading

condition corresponds to an intermediate case, with a transverse metacentric height GM = 1.3 meters, and a draft of 13.1 meters.

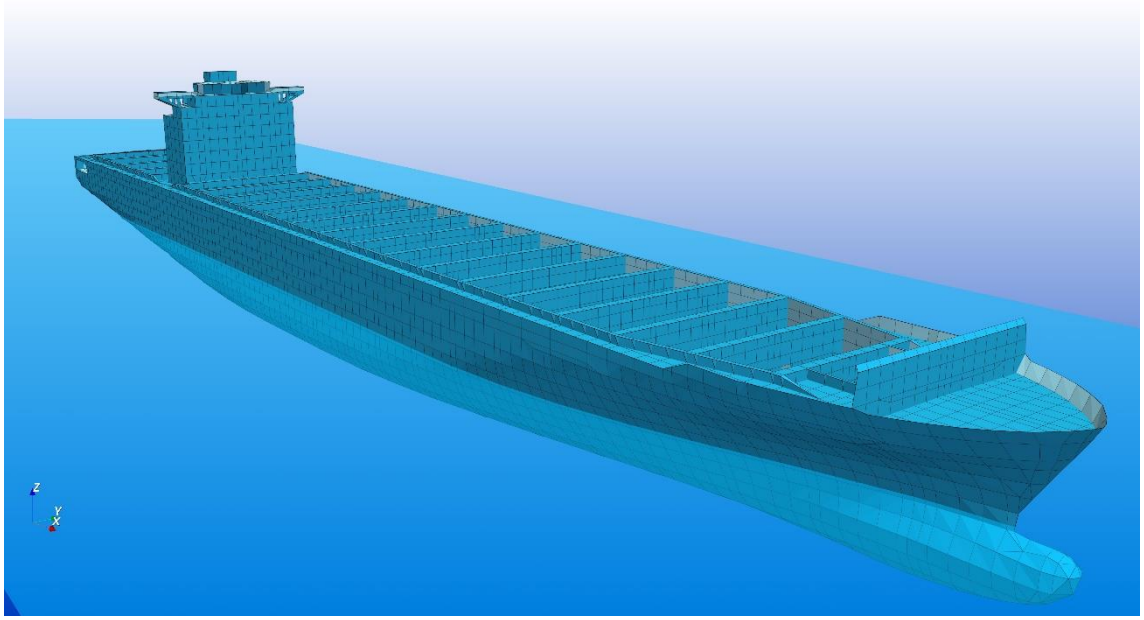

Figure 4. Full length finite element model of the ship

This coarse mesh (see Figure 4) is deemed precise enough to get global deformations, including strains in LBSG, which are recovered by computing the stresses in rod elements placed at the relevant locations.

However, a much finer resolution is needed to access the local strains, particularly for fatigue assessment. The fine meshes created to recover the stresses in the strain gauge locations are presented in Figure 5. The fine meshes contain around 4 300 elements, with a typical element size of 25 mm around hatch corner sensors.

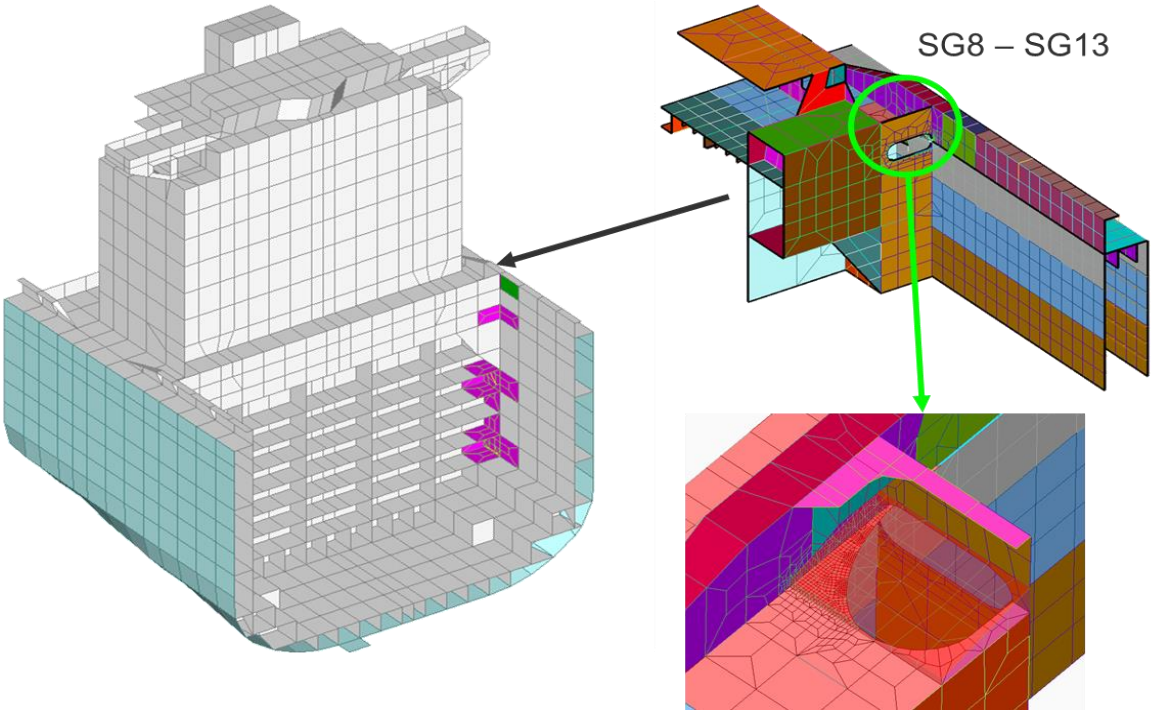

Figure 5. Finite element model of the hatch corners

A top-down procedure is used to recover stresses in the detail fine meshes. Coarse mesh deformations are applied to the boundaries of detail mesh and the local stress is recovered from the closest element to the local strain gauge position. Special care is taken for the modelling of the complex hatch corner area, and rod elements are placed along the free edge to recover stresses comparable to those measured by the strain gauges.

III – 2 Hydrodynamic modeling

The details of the boundary integral equation method used to solve the seakeeping with forward speed are briefly recalled here, and more details can be found in [1].

Within the framework of the potential flow theory, the boundary value problem is closed by the boundary conditions at the body, free surface and infinity, which ensure the continuity of the fluid kinematics and hydrodynamic pressures. The main difficulty comes from the free surface condition, which becomes extremely complex when the ship advances with forward speed, making it incomparably more difficult to solve the boundary value problem with forward speed compared to the zero-speed case. In particular, the interaction of the steady and unsteady flow components must be accounted for consistently. In frequency domain, the linearized free surface condition for the unsteady velocity potential φ can be written:

$$\varphi_z - \omega^2\varphi - 2i\tau\mathbf{w}\cdot\nabla\varphi + F_r^2\mathbf{w}\cdot\nabla(\mathbf{w}\cdot\nabla\varphi) + F_r^2\nabla\varphi\cdot(\mathbf{w}\cdot\nabla)\mathbf{w} + \bar{\Phi}_{zz}(i\tau\varphi - F_r^2\mathbf{w}\cdot\nabla\varphi) = 0 \quad (1)$$

Where ω denotes the dimensionless encounter frequency $\omega = \omega_e/\sqrt{gL}$, F_r the Froude number $F_r = U/\sqrt{gL}$ and τ the Brard number $\tau = \omega F_r$. The notation $\mathbf{w}$ is used to denote the unitary steady velocity potential $\mathbf{w} = \nabla\bar{\Phi} - \vec{\imath}$, which corresponds to the ship advancing with unit forward speed in calm water.

To highlight the complexity, the free surface condition for the problem without forward speed is only written as:

$$\varphi_z - \omega^2\varphi = 0 \quad (2)$$

In the approach proposed in [1], the so-called Kelvin Green's function is used, satisfying the radiation condition at infinity and fully linear free surface conditions. Only a small zone on the free surface close to the ship must be modelled (as shown in Figure 6).

One of the difficulties of this new method being the evaluation of the spatial derivatives of the velocity potential, a specific meshing strategy is used: the input mesh consists in high order (quadratic) panel, that are then subdivided into nine sub-patches; the solution of the velocity potential is then obtained at the center of each sub-patch, assuming a constant distribution over the sub-patch.

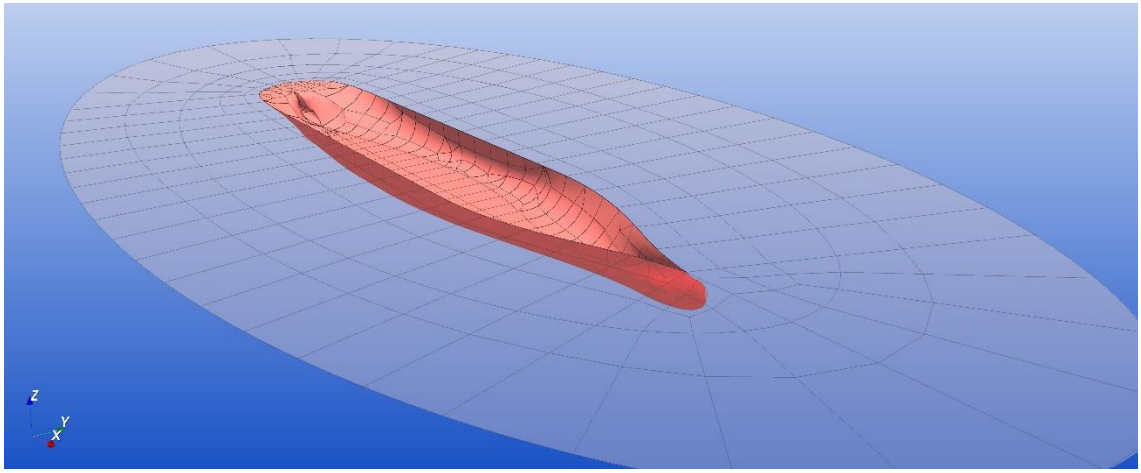

Figure 6. Hydrodynamic mesh of the ship and free surface

III – 3 Hydro-structure interface

The pressures computed on the hydrodynamic mesh are then mapped onto the structural model. The mapping algorithm and its implementation are explained in [2]. The hydrodynamic coefficients used to solve the seakeeping problem (added masses, radiation damping, diffracted and incident wave loads) are then obtained by integration the pressures directly onto the structural model. To verify the hydro-structure mapping, the hydrodynamic coefficients integrated over the structural model can be compared with those integrated over the hydrodynamic model, as shown in Figure 7 for the excitation forces computed for a 60° wave direction (more comparisons can be found in [2]).

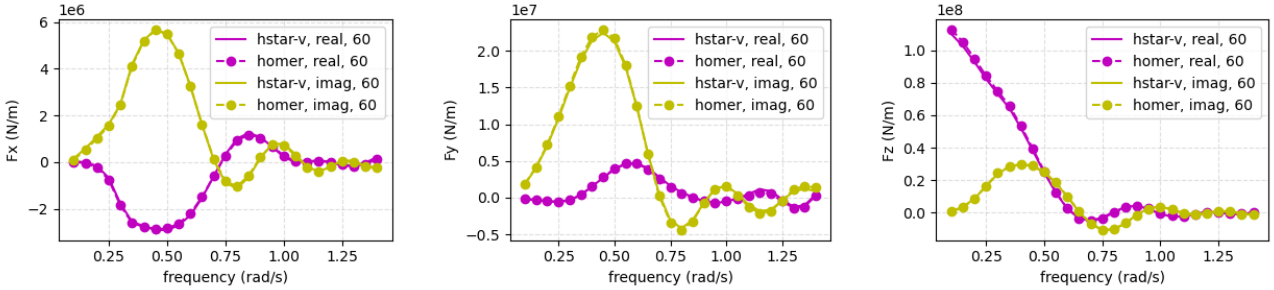

Figure 7. Comparison of real and imaginary parts of wave forces integrated on the structural model (*homer*) and on the hydrodynamic model (*hstar-v*)

Once the seakeeping problem has been solved and the motions computed, the hydrodynamic pressures and inertia loads are transferred to the finite element solver in the same manner as when working with the classical seakeeping solution [4]. The stress transfer functions are then obtained and will be used in a spectral analysis to compute the structural response of the ship to the sea states encountered.

IV – Overview of data

IV – 1 Availability of data

The data is a priori available from January 2011 to May 2019. However, the actual availability of data can vary quite a bit: sometimes the sensors are not measuring anything. Furthermore, the measurement data is not always perfect, and pre-processing is necessary to ensure that the comparisons will be made using reliable data only. The following filters are applied to the data:

- Time-windows for which ship speed is lower than 10 knots are removed. These time-windows correspond to periods where the ship is in port and recordings mainly correspond to noise but also to times when ships is performing maneuvers or sailing at low speeds.
- Time windows corresponding to non-stationary navigation conditions are removed: excessive variation of speed, course, GPS position. The reason for this is that it is impossible to account for this type of effect in the spectral analysis. This is performed by limiting standard deviation of a given measurement parameter
- Time-windows for which one or more LBSG are obviously not measuring anything (or only noise) are removed.
- Time-windows for which non-physical data are identified on at least one strain gauge are removed.

All in all, after applying these quality-checks, the number of 1-hour time windows available for a fair comparison is reduced. Combining all criteria leaves approximately 21% of the measurement periods ready for comparison.

IV – 2 Wave data

The ERA 5 hindcast database was used to retrieve the wave data along Rigoletto's trajectory, using the GPS records (see Figure 8). The data was obtained from the Climate Data Store provided by the ECMWF via the Copernicus Climate Change Service [5]. This dataset is freely available online and consists of hourly outputs from 1979 to the present and covers the entire globe.

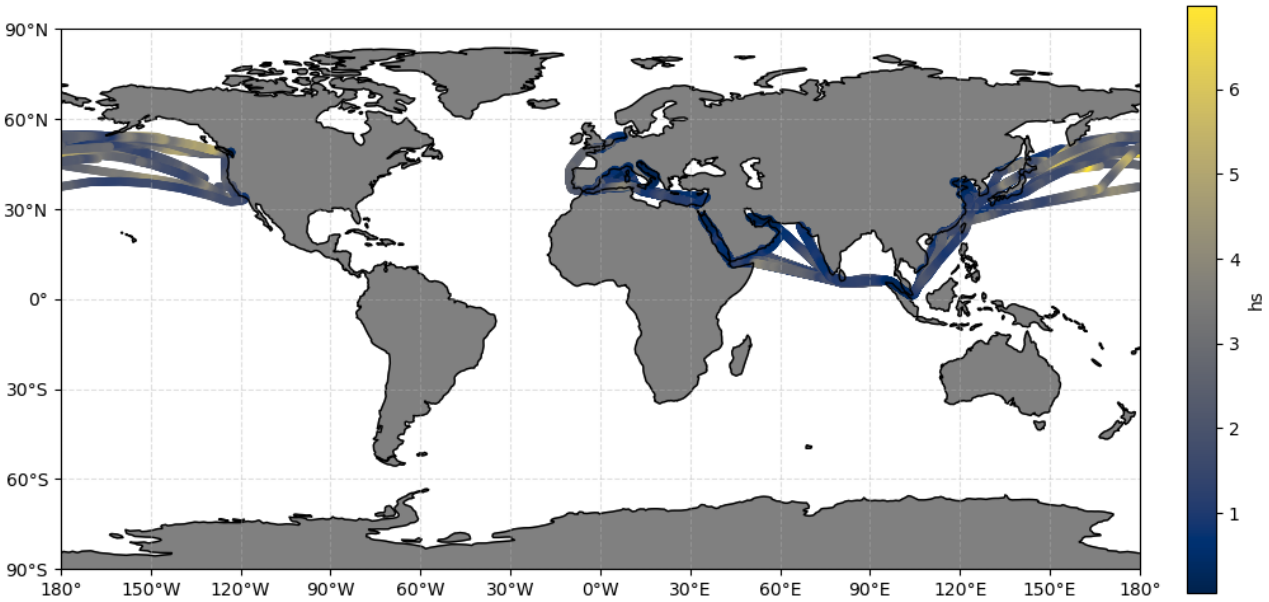

Figure 8. GPS records of the CMA CGM Rigoletto, colored by significant wave height

The full wave spectra were retrieved at the locations of interest. The wave spectra are discretized using 24 directions and 30 frequencies between 0.2 and 3.4 rad/s. The main values (significant wave height Hs, peak period Tp, mean wave direction) are shown in Figure 9.

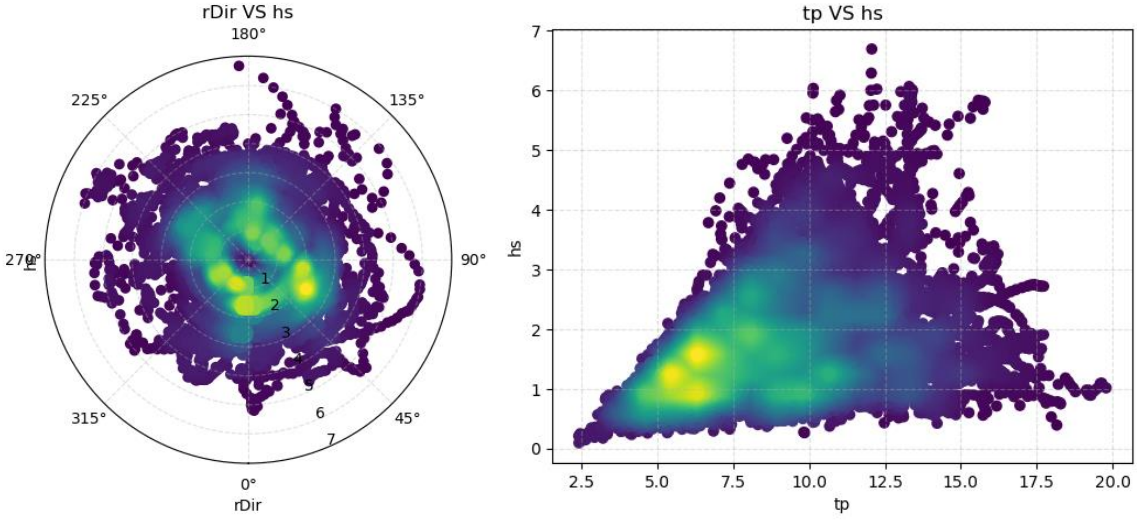

Figure 9. Relative wave directions, significant wave heights and peak periods

V – Results

V – 1 Methodology for the comparisons

The results of the hydro-structure computations are compared with the measurements in terms

of cumulative fatigue damage, using the recommended practice [6].

On the measurement side, the stress cycles are counted using a Rainflow method for each one-hour time window, and the cumulative damage is then computed using the Palmgren-Miner's rule. As the aim of this study is not to compute an actual damage but to compare two sets of data, a standard single slope SN curve is used for all locations, with $K = 1.52 \cdot 10^{12}$ and $m = 3$.

On the computation side, the response spectrum is computed using the transfer functions and the wave spectrum obtained from the hindcast database. Assuming a narrow-banded spectrum, the damage can then be computed using a closed-form expression.

In all figures below, the results obtained with the classical seakeeping solution are displayed with the "*Hydrostar-ref*" label, and the results obtained with the new solution are displayed with the "*Hydrostar-V*" label.

V – 2 Comparison of global stresses at deck level

The comparison of fatigue damages computed from the stresses at deck level display a different behavior for the two instrumented frames. At frame 100 (close to midship), the two seakeeping solutions give approximately the same results (Figure 11), which match very well with the measurements. At frame 75 however (close to the engine room bulkhead), the classic seakeeping solution overestimates the damage, while the new seakeeping solution displays a very good match with the measurement (Figure 10).

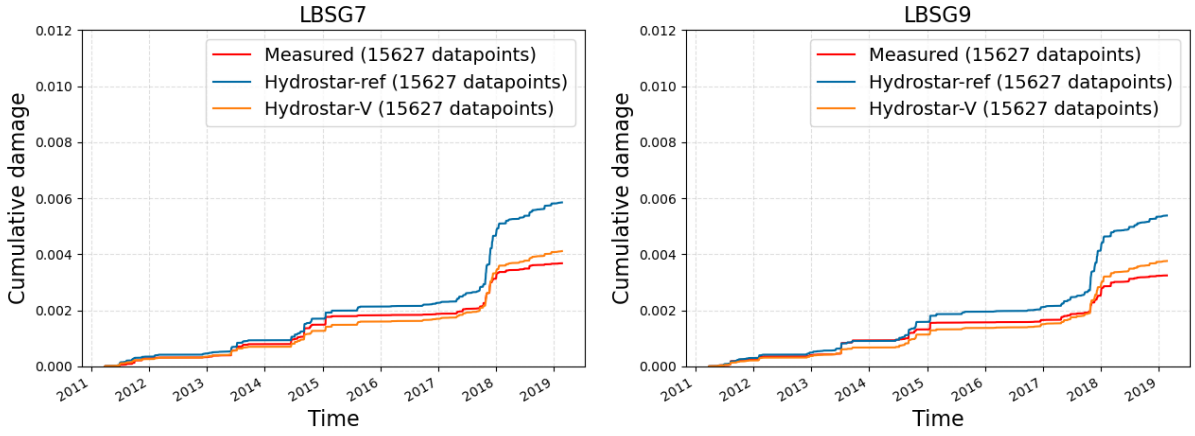

Figure 10. Fatigue damage at frame 75, at deck level (portside and starboard)

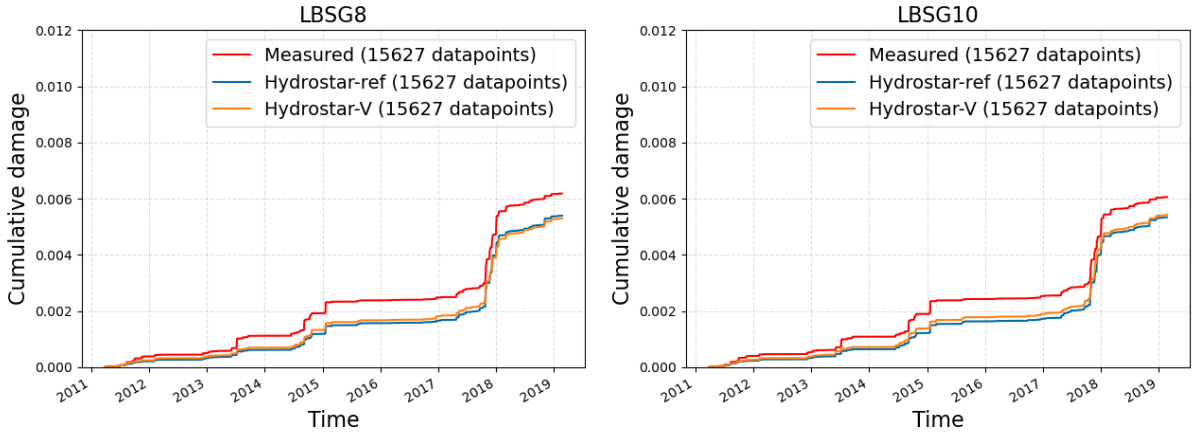

Figure 11. Fatigue damage at frame 100, at deck level (portside and starboard)

The results are then clustered, depending on the operating conditions:

- GM below and above three meters, to distinguish the conditions approximately matching the GM of the model
- Relative wave directions, with 45° angular sector for each cluster

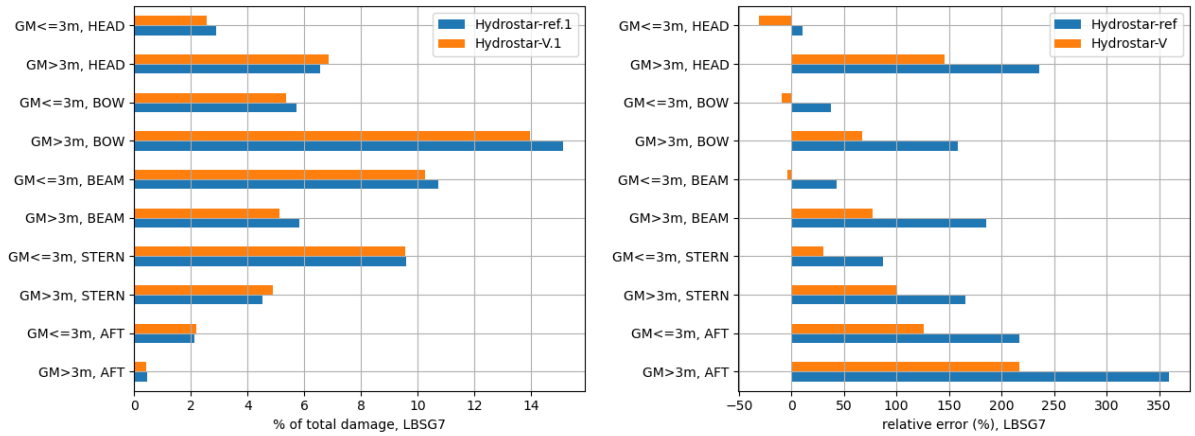

Figure 12. Distribution of damages and relative errors for LBSG7 (Frame 75, portside)

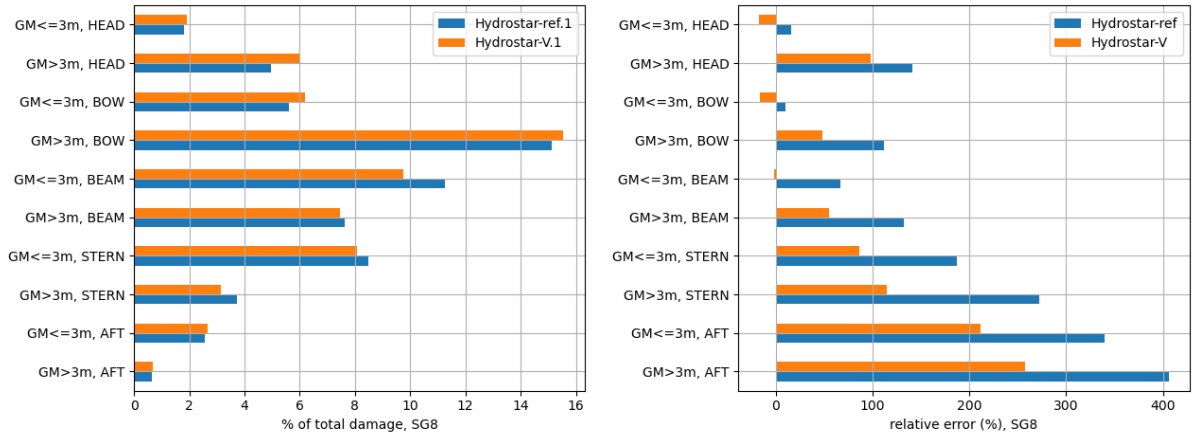

Figure 13. Distribution of damages and relative errors for LBSG8 (Frame 100, portside)

The pictures above (Figure 12 and Figure 13) then show on the left side the percentage of damage coming from each cluster, and on the right side the error made by the two seakeeping models compared to the measurements. On frame 75 (see Figure 1Figure 12), the error is decreased for all conditions, except when GM is less than 3 meters and for head waves; this explains that the overall precision is much better, as shown previously. On frame 100 (see Figure 13), the two models give roughly the same errors. For all four LBSGs, the error made on aft waves is always quite large but does not impact the overall performance because of the very low contribution to the total damage (less than 3%).

V – 3 Comparison of global stresses at the bottom of the cargo holds

The comparison of fatigue damages computed from the stresses at the bottom of the cargo holds displays an overall bad match, overestimating the total damage somewhere between 50 and 100%, as shown in Figure 14and Figure 15. The same limits have been chosen for the y axis to highlight the lower stress levels measured (and computed) at Frame 75 compared to Frame 100.

The same clustering as before is performed with respect to GM values and to relative wave directions. Figure 16 and Figure 17 both show the same behavior, with an overall poor performance (high relative errors), and no significant increase when using the new seakeeping solution

(Hydrostar-V). This overestimation is consistently observed for all sensors at the bottom of the cargo holds, hinting in the direction of a bad representation of the actual arrangement of LBSG and surrounding structure with respect to the finite element model.

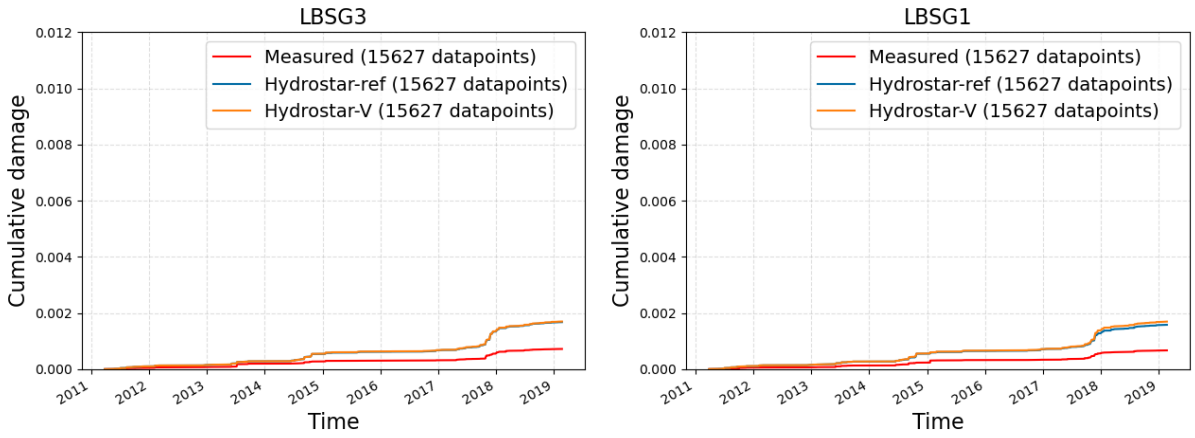

Figure 14. Fatigue damage at frame 75, at the bottom of the cargo hold (portside and starboard)

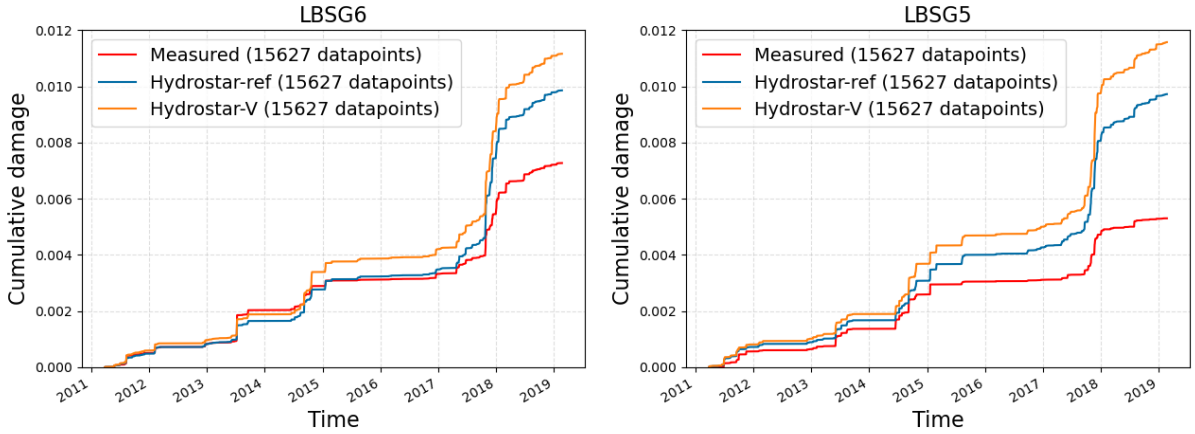

Figure 15. Fatigue damage at frame 100, at the bottom of the cargo hold (portside and starboard)

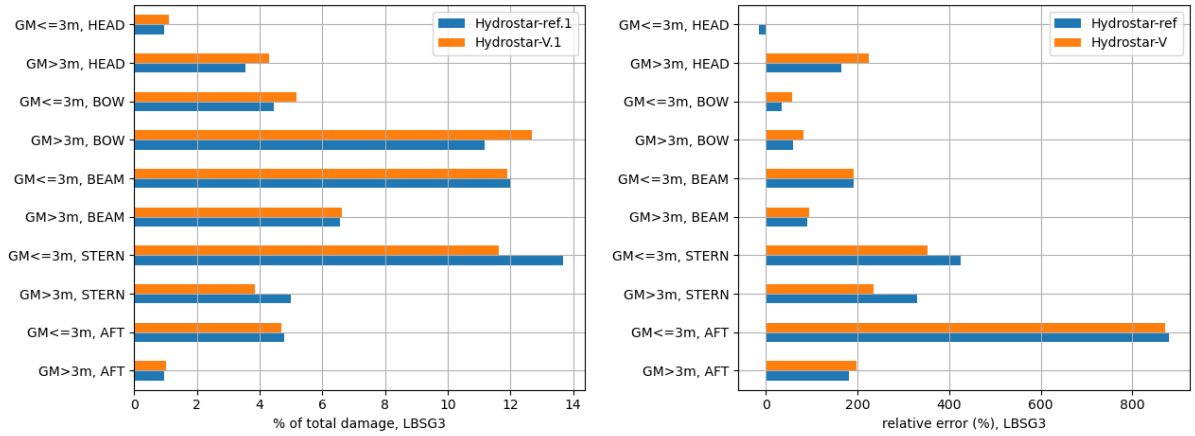

Figure 16. Distribution of damages and relative errors for LBSG3 (Frame 75, portside)

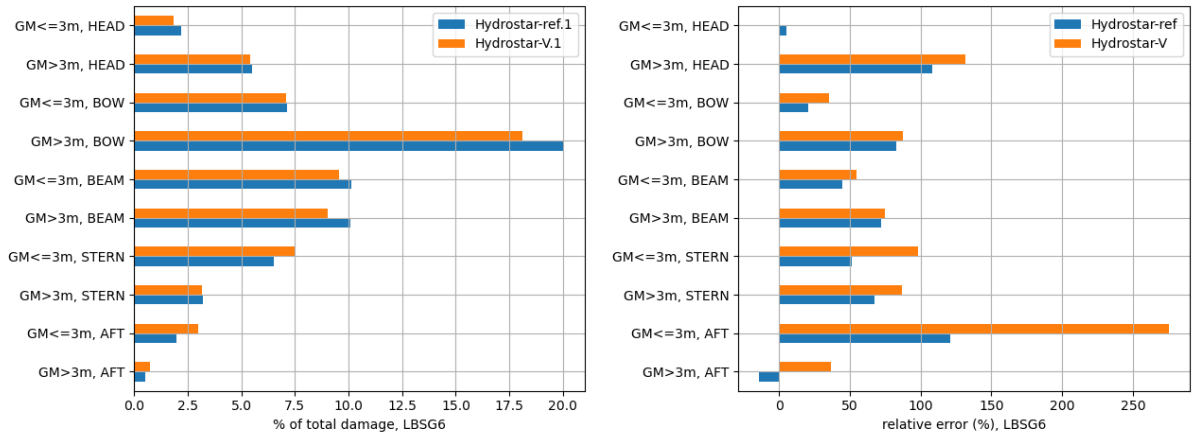

Figure 17. Distribution of damages and relative errors for LBSG6 (Frame 100, portside)

V – 4 Comparison of local stresses at hatch corners

Mirroring the patterns observed for the stresses computed at frame 75 and deck level, the comparison of damages computed from stresses at the hatch corners between the main deck and the engine room bulkhead (both on portside and starboard, see Figure 18) displays a much better match of the new seakeeping solution with the measurements compared to the classical seakeeping solution.

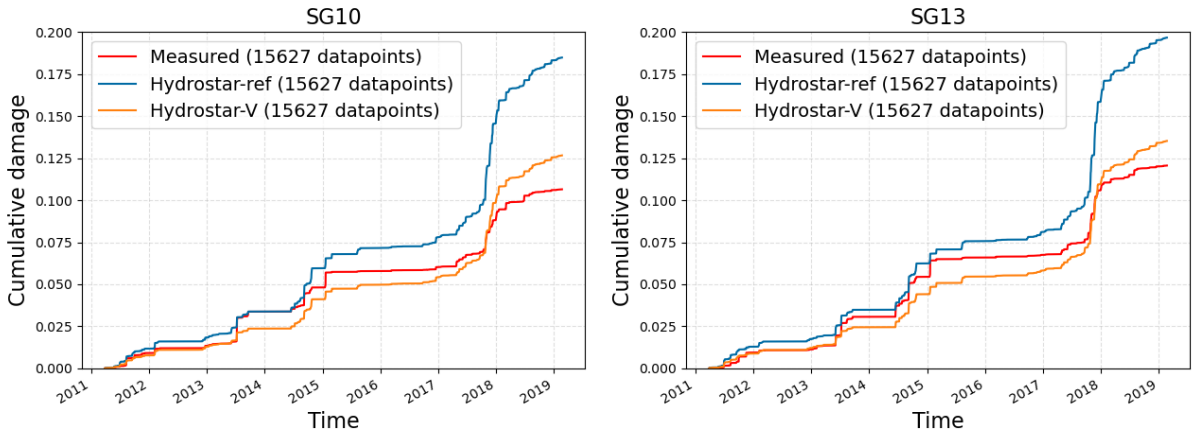

Figure 18. Fatigue damage at hatch corners between the main deck and the engine room bulkhead

As for the LBSGs at deck level at frame 75, the clustering of the data with respect to GM values and to the relative direction of incoming waves shows that the new solution is more precise for all the conditions (Figure 19).

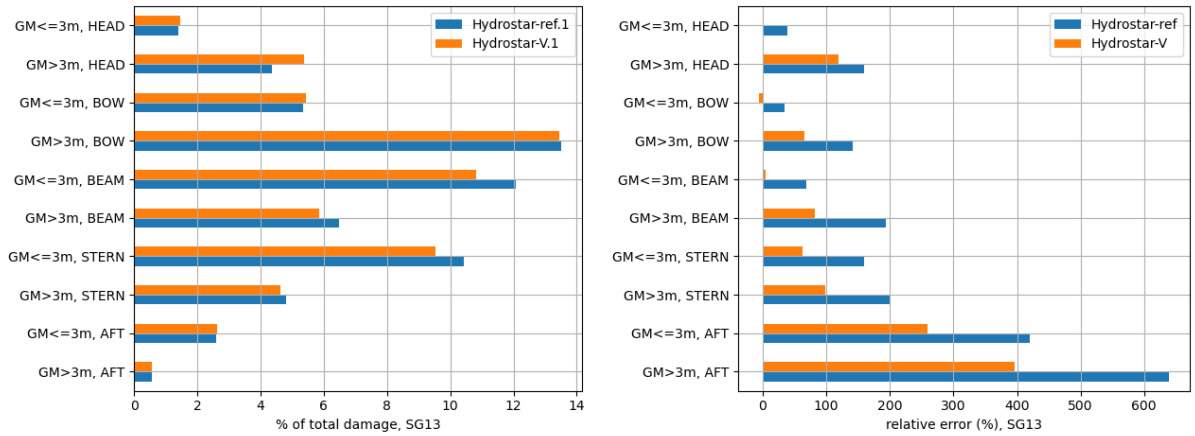

Figure 19. Distribution of damages and relative errors for SG13 (Frame 75, starboard)

VI – Conclusion

After many years of research and development, the recent progress towards a consistent solution of the forward speed seakeeping problem have made it possible to improve the computation of stress transfer functions for ships sailing with high forward speeds ([1] and [2]). In parallel, the large amount of accumulated full-scale measurements aboard a 9400 TEU container ship have created a database suitable for the validation of hydro-structure computations.

The comparisons presented in this paper show that the use of a more advanced seakeeping solution allows for a better evaluation of stresses at the connection between the main deck and the engine room bulkhead (for both global deformations and stresses in critical structural elements), which is of paramount importance for ultra large container ships. The stresses computed at midship are not affected by the change of seakeeping solution and are accurately predicted by both methods. Some uncertainties remain for the comparisons of the stresses at the bottom of the cargo holds, where the stresses are still overestimated; these could be linked to a too coarse modeling of this part of the structure in the finite element model of the ship used for the analyses.

It is also interesting to notice that for both seakeeping solutions, the error is always worse for metacentric heights above 3 meters, which are farther away from the GM of the loading condition used in the structural model of the ship (1.3 meters). This is to keep in mind when performing this kind of comparison against full scale measurement data, and it speaks in favor of using several loading conditions whenever possible.

Acknowledgments

This work was carried out for the CONVIRT working group of the Cooperative Research Ships (CRS: www.crships.org) and was made possible by many years of collaborative research within the CRS framework, mainly during the CRISM and iShip working groups. The author would like to thank all the partners of these projects, for allowing the publication of this work, and above all for the fruitful collaboration that made these analyses possible.

References

[1] Chen, Nguyen, Ten, Ouled Housseine, Choi, Diebold, Malenica, de Hauteclocque & Derbanne. “New seakeeping computations based on potential flows linearized over the ship-shaped stream”. In *Proceedings of the 15th international symposium on practical design of ships and other floating structures (PRADS)*, 2022.

[2] Nguyen, de Hauteclocque, de Lauzon, Malenica & Chen. “Quasi-static fluid structure interactions for ships advancing in waves with constant forward speed”. In *Proceedings of the ASME 43rd international conference on ocean, offshore and arctic engineering (OMAE)*, 2024.

[3] Koning & Kapsenberg. “Full scale container ship cross section loads – first results”, In *Proceedings of the 6th International Conference on Hydroelasticity in Marine Technology (HYEL)*, 2012.

[4] Malenica, Derbanne, Sireta, Tiphine, de Hauteclocque & Chen. “HOMER – integrated hydro-structure interactions tool for naval and offshore applications”. In *Proceedings of the International Conference on Computer Applications in Shipbuilding (ICCAS)*, 2013.

[5] Hersbach, Bell, Berrisford, Biavati, Horányi, Muñoz Sabater, Nicolas, Peubey, Radu, Rozum, Schepers, Simmons, Soci, Dee & Thépaut, *ERA5 hourly data on single levels from 1940 to present.,* 2023.

[6] Bureau Veritas. *NI 611: Guidelines for fatigue assessment of ships and offshore structures.* 2020.